Efficient View Frustum Culling

Daniel Sýkora
sykorad@fel.cvut.cz

Josef Jelínek
jelinej1@fel.cvut.cz

Department of Computer Science
Faculty of Electrical Engineering
Czech Technical University
Prague / Czech Republic

1. Abstract

We have implemented efficient algorithms for view frustum culling introduced in the article *Optimized View Frustum Culling Algorithms for Bounding Boxes* [1] by *Ulf Assarson* and *Thomas Möller* (2000). We measure and evaluate the efficiency of selected speed-up techniques used in static and dynamic scenes.

Keywords: view frustum culling, bounding volumes, scene hierarchy.

2. Introduction

The main idea how to make VFC efficient was invented by *Clark* [2] who used scene hierarchy. *Slater* and *Chrysanthou* [3] developed VFC probabilistic caching scheme which is significantly faster but in some cases produces unacceptable errors. Lots of improvements based on traversal coherency of the scene hierarchy were also presented by *Bittner* and *Havran* in [4].

We have examined the article *Optimized View Frustum Culling Algorithms for Bounding Boxes* [1] and also the following technical report by the same authors *Optimized View Frustum Culling Algorithms* [5] which presents generalized and detailed parts of the basic article.

In this section we will describe briefly the main novel ideas of optimization methods that *Assarson* and *Möller* introduced in [1]. The following explanation is also used as the basic information about our implementation of the presented methods. We will also include a detailed description, critical comments and remarks about changes in our implementation. The presentation of the abilities of our application will take place in *Section 3* including the discussion about the results in *Section 4* and *5*.

2.1 Motivation and results in [1]

The main goal was to speed-up the elimination of the invisible objects in complex scenes from the rendering pipeline. This part of code may not be crucial in most cases but its speeding up will help especially in huge scenes.

Moreover the general methods the authors of [1] present also speed-up techniques which use low degree of freedom of the camera motion in the user-driven walk-through the scene. This is significant for well known 3D computer games driven by a player from his own point of view.

All methods are independent each other. It is possible to determine stand-alone success in comparison with another VFC algorithms. *Möller et al.* used the VFC algorithms of *DirectModel* (*DirectModel 1.0 Specification, Hewlett Packard*) and *Cosmo3D* (*Cosmo3D programmers' guide, Silicon Graphics Inc.*) as a measure ethalon for establishing presented speed-ups.

All measurements were performed for several types of bounding volumes and their hierarchy in scenes consisting of about 150 thousands of polygons. They provide a solution which is 3–10 times faster than *DirectModel* a system that uses the axes aligned bounding boxes hierarchy, and 1.2–1.4 times faster than Cosmo3D with the hierarchy of bounding spheres.

2.2 Camera, bounding volumes and hierarchy

We could reduce the whole problem of elimination of invisible objects to the test of the collision of two volume objects: the visible volume of a camera, also known as the *viewing frustum*, and the bounding volume of the current object.

The visible volume of the camera is represented by six planes. Two of them (*near* and *far*) are parallel. The other four are connected in one point of space that represents the viewpoint. They inclined a spatial angle that represents the FOV *field of view* of camera. The *far* plane bounds visibility of far objects in space. The *near* plane determines the distance of the view-port from the viewpoint.

Möller et al. specify the VF (*viewing frustum*) as an axes symmetrical quadrilateral frustum. Often the reduced versions of the viewing frustum without the *far* plane and sometimes without the *near* plane are used in practice. The *near* plane of VF could be changed to the spherical surface in cases when we need to render objects in a panoramatic projection.

The most commonly used bounding volumes for the VFC are already mentioned AABBs and spheres, but also the OBB (*oriented bounding box*) or the k-DOP (*discrete oriented polytope*) [7]. The volume of the object in proportion to the volume of its bounding solid determines the conservativity of the elimination algorithm. The closer are the volumes the harder is the implementation of such a VFC algorithm. The VFC algorithm based on bounding spheres is simple and fast. That is the reason for no really significant speed-up improvements as is shown on the results in [1].

The most commonly used structure that is good compromise between the tight-fitting k-DOPs and conservative spheres is the AABB. The important property of the AABB is aligning to the world coordinates. In contrast to the OBB, that is transformed by the same matrix as the vertices of the bounded volume, many transformations can be removed in the case of AABB. Still there is need to transform the AABB if the object rotates. Good compromise for this case can be a combined hierarchy of the bounding boxes. There are the OBBs in leafs of the oriented acyclic graph of the scene, from which the AABBs on the higher levels of the hierarchy can be easily computed only by a transformation and by finding the bounds of the eight vertices set.

Clark [2] shown that the scene hierarchy is really important data structure that helps speeding up the VFC significantly. *Möller et al.* obtain the best results for speeding up the eliminating phase with the hierarchy of the AABB. The more complex hierarchy with the k-DOP elements was not used by the authors, but most of the optimization ideas can be used even for these complex structures.

There should be noted that the authors did not describe the way how the AABB hierarchy was created, its implementation, how and how often they refreshed the dimensions of the bounding volumes, whether the scenes consisted of some animated solids etc.

2.3 Basic VFC algorithm

Although *Möller et al.* mentioned the system with VFC algorithm that they used as the base for the comparison, but they did not give any further details. They only stated that *DirectModel* uses the general test of the collision of two AABBs. There was not mentioned its conservativity only the way how to convert the test of the axes aligned box to the quadrilateral frustum.
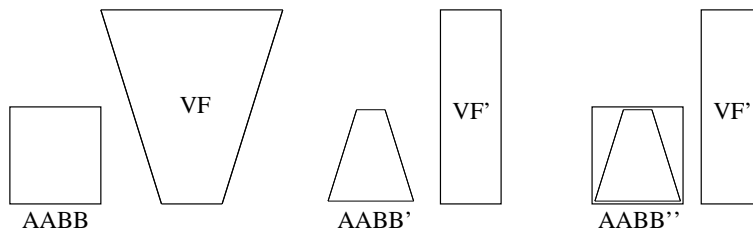

Figure 1: Transformation of the AABB and VF to AABBs.

The entire procedure is in *Figure 1*. The AABB and the VF is transformed by the perspective transformation that reduces the VF to a box. This transformation needs 72 multiplications. The new AABB is constructed around the original VF. The collision detector is applied on this couple and can be realized by the six comparisons.

An important feature of the basic algorithm is its conservativity in the sense of the detection of the state where the bounding volume intersects the visibility volume of the camera. Low precision of this test can cause unnecessary culling of a big amount of triangles of an object inside the bounding volume. For an objective comparison of methods with different conservativity the global time measurement is needed because the results of the VFC in this case affects the load of the output device that can be hardware accelerator or software renderer.

Considering that we did not have all details of the implementation of the same basic VFC algorithm for comparison as the authors of the article, we have used another much less expensive in the term of time that has the same conservativity as the so called *Assarson-Möller's* basic test (*basic intersection*) that will be described later. The acceleration can be correctly measured even on less complex scenes by comparison of the CPU needed to compute only the VFC test routines. But we have compared the algorithms with same which producing the same results. The fact that the *Möller et al.* do not take care about conservativity of the compared algorithms affects reliability of the presented results.

The idea of the basic VFC algorithm for comparison is taken from the article *Improved frustum-object cull* [6] where *Villi Miettinen* gives many experiences with the practical applications for solving the VFC problem. His algorithm is optimized for AABB and uses one of the *Assarson-Möller's* optimization. We used only the core of *Miettinen's* test without this additional optimization.

The *Miettinen's* basic VFC algorithm uses the collision detection between the VF and a sphere. In this case the bounding sphere is determined by the center of the AABB and a half of the diagonal connecting the minimal and the maximal vertex of the AABB. So it is sufficient to compute only the distance of the center of the AABB from the tested plane and consists of one dot product and the comparison to the radius of the bounding sphere.
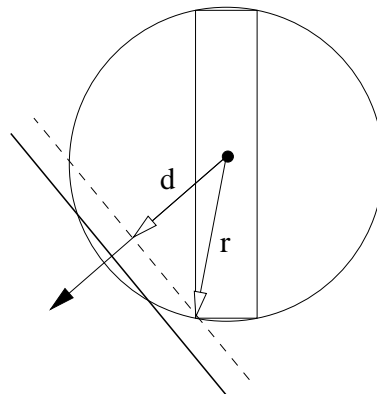

Figure 2: Basic VFC algorithm idea.

Figure 2 demonstrates the fact that the conversion of the AABB to the bounding sphere is not exact. If we measure the entire radius of the sphere and the distance from the center of the AABB we can see that we only need to compare its projection to the direction of the normal vector of the tested plane. There is one more dot product compared with the simple sphere-plane test. The following pseudo-code describes more implementation details of this method:

```
int AABBvsFrustum(AABB *b, FRUSTUM *f)
{
 float m, n; int i, result = INSIDE;

 for (i = 0; i < 6; i++) { PLANE *p = f->plane + i;

    m = (b->mx * p->a) + (b->my * p->b) + (b->mz * p->c) + p->d;
    n = (b->dx * fabs(p->a)) + (b->dy * fabs(p->b)) + (b->dz * fabs(p->c));

    if (m + n < 0) return OUTSIDE;
    if (m - n < 0) result = INTERSECT;

    } return result;
}
```

Vector (mx, my, mz) represents the center of the AABB. Absolute values of the normal vector of the plane (a, b, c) transform all possible values to the first octant so its dot product with the vector representing a half of the AABB diagonal (dx, dy, dz) will be always positive.

Three different values are possible as the output of the test that determines the continuation of the rendering pipeline.

- OUTSIDE: Bounding box is totally outside of the VF so the bounded volume is also outside. The object or the dot hierarchy is eliminated from the further processing.
- INSIDE: Bounding box is totally inside of the VF. There is no need for further culling of the geometry of the bounded object or down traversal the hierarchy. This state is also useful information for the software renderer that could avoid the low-level polygon clipping.

- **INTERSECT**: Object could intersect the VF. The down traversal the hierarchy is needed and in the case of leafs the sending of the entire object for culling on the level of the object geometry.

Accuracy of reporting **INTERSECT** value depends on the conservativity of the used method. Beside the inaccuracy caused by the size of the AABB and the size of the bounded object there are another inaccuracies in the corners of the VF. The algorithm detects the **INTERSECT** state even when the bounding volume is in fact outside the VF. This case is displayed on *Figure 3* where the regions of failure of the algorithm are in edges of sweep frustum.
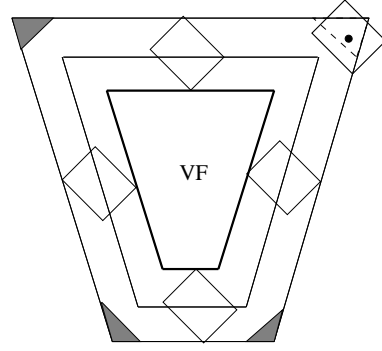

Figure 3: VFC algorithm inaccuracy.

2.4 Basic intersection test

The first optimization in the article is the basic test (*basic intersection*) of the collision of the AABB with the VF. Instead of finding out locations of all vertices in relation to the tested plane, it is possible to determine one of the AABB states (**OUTSIDE**, **INSIDE**, **INTERSECT**) only by the test of two vertices: the n-vertex and the p-vertex.

Figure 4 explained the geometric meaning of n,p-vertices. They are defined in the following way: the farthest vertex of the AABB in the positive resp. negative sense in the direction of the normal vector of the plane is the p-vertex resp. n-vertex. Because of the geometry of the AABB it is possible to reduce the determining of the n and p-vertices using look-up *Table 1*. This table is indexed by the signs of the normal vector parts of the given VF plane.
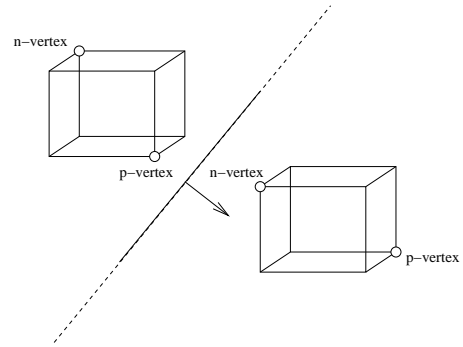

Figure 4: Examples of n,p-vertices.

n_x	n_y	n_z	p-vertex	n-vertex
+	+	+	$[x_{max}, y_{max}, z_{max}]$	$[x_{min}, y_{min}, z_{min}]$
+	+	−	$[x_{max}, y_{max}, z_{min}]$	$[x_{min}, y_{min}, z_{max}]$
+	−	+	$[x_{max}, y_{min}, z_{max}]$	$[x_{min}, y_{max}, z_{min}]$
+	−	−	$[x_{max}, y_{min}, z_{min}]$	$[x_{min}, y_{max}, z_{max}]$
−	+	+	$[x_{min}, y_{max}, z_{max}]$	$[x_{max}, y_{min}, z_{min}]$
−	+	−	$[x_{min}, y_{max}, z_{min}]$	$[x_{max}, y_{min}, z_{max}]$
−	−	+	$[x_{min}, y_{min}, z_{max}]$	$[x_{max}, y_{max}, z_{min}]$
−	−	−	$[x_{min}, y_{min}, z_{min}]$	$[x_{max}, y_{max}, z_{max}]$

Table 1: Look-up table for determining the n and p-vertices.

The basic test uses only two dot products. The first one detects if the n-vertex is outside the half-space defined by actual VF plane. In this case the AABB is also outside VF. If the test fails the next test of the p-vertex is processed. If it is outside then the AABB intersects the plane. In the opposite case the AABB is inside the half-space. The whole algorithm of this basic test is described in the next pseudo-code listing.

Index-vectors (nx, ny, nz) and (px, py, pz) gain *min* and *max* vertices. The implementation of the *Table 1* is reduced to 6 values that are used for indexing of the table of two items with the minimal and maximal parts of the AABB coordinates. The test for the **OUTSIDE** state can be done only by one dot product.

```
int AABBvsFrustum(AABB *b, FRUSTUM *f)
{
 float m, n; int i, result = INSIDE;

 for (i = 0; i < 6; i++) { PLANE *p = f->plane + i;

     m = (p->a * b->v[p->nx].x) + (p->b * b->v[p->ny].y) + (p->c * b->v[p->nz].z);
     if (m > -p->d) return OUTSIDE;

     n = (p->a * b->v[p->px].x) + (p->b * b->v[p->py].y) + (p->c * b->v[p->pz].z);
     if (n > -p->d) result = INTERSECT;

     } return result;
}
```

2.5 Plane masking and coherency

The next two optimization have the best effect on the speed: *plane masking* and using the *plane coherency* of the VFC between frames (*temporal coherency*).

To take advantages of the hierarchy the authors invented an incremental reduction of planes that are needed to test for collision with the AABB in the given level of hierarchy. If the parent bounding box is inside the half-space then this test is not needed in lower levels of the hierarchy. Each child is then also inside this half-space. See *Figure 5*.

In the recursive traversal the bit-mask of the planes is sent from a parent to its children. In the position of the second dot product that is used for determining the INTERSECT state the plane is masked out in the case of the negative test for the elimination of further tests on the next levels of the hierarchy.
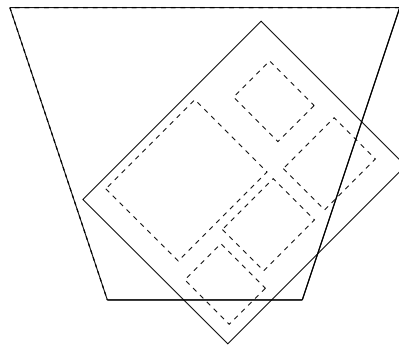
Figure 5: Plane masking.

```
int AABBvsFrustum(AABB *b, FRUSTUM *f, int in_mask, int *out_mask)
{
 float m, n; int i, k, result = INSIDE; *out_mask=0;

 for (i = 0, k = 1; k <= in_mask; i++, k += k) if (k & in_mask) {

     PLANE *p = f->plane + i;

     m = (p->a * b->v[p->nx].x) + (p->b * b->v[p->ny].y) + (p->c * b->v[p->nz].z);
     if (m > -p->d) return OUTSIDE;

     n = (p->a * b->v[p->px].x) + (p->b * b->v[p->py].y) + (p->c * b->v[p->pz].z);
     if (n > -p->d) { *out_mask |= k; result = INTERSECT; }

     } return result;
}
```

The *plane coherency* optimization provides both theoretically and practically the highest acceleration of the current VFC algorithm. This method used the temporal coherency that cause little changes of the configuration of the VF and AABBs. It is very likely that if a test with a plane fails then it fails also in the next frame with the same plane. So it is sufficient to remember the index of the last tested plane and begin with this test in the next frame. One more item in the AABB structure is then needed where

this plane index is stored. Also the modification of the algorithm is needed to use both tests together correctly. This situation is shown in *Figure 6* where the re-ordering of the plane tests depending on the tests in the previous frame.
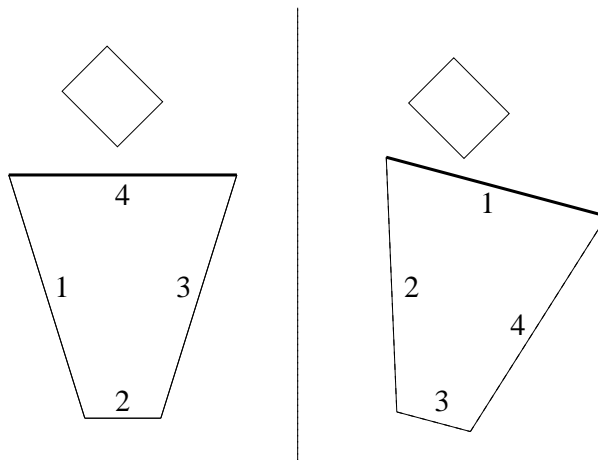

Figure 6: The plane index renumbering in the *plane coherency* method.

```
int AABBvsFrustum(AABB *b, FRUSTUM *f, int in_mask, int *out_mask)
{
 float m, n; int i, k = 1 << b->start_id, result = INSIDE;

 PLANE *sp = f->plane + b->start_id; *out_mask=0;

 if (k & in_mask) {

    m = (sp->a * b->v[sp->nx].x) + (sp->b * b->v[sp->ny].y) + (sp->c * b->v[sp->nz].z);
    if (m > -sp->d) return OUTSIDE;

    n = (sp->a * b->v[sp->px].x) + (sp->b * b->v[sp->py].y) + (sp->c * b->v[sp->pz].z);
    if (n > -sp->d) { *out_mask |= k; result = INTERSECT; }

    }

 for (i = 0, k = 1; k <= in_mask; i++, k += k)

    if ((i != b->start_id) && (k & in_mask)) { PLANE *p = f->plane + i;

       m = (p->a * b->v[p->nx].x) + (p->b * b->v[p->ny].y) + (p->c * b->v[p->nz].z);
       if (m > -p->d) { b->start_id = i; return OUTSIDE; }

       n = (p->a * b->v[p->px].x) + (p->b * b->v[p->py].y) + (p->c * b->v[p->pz].z);
       if (n > -p->d) { *out_mask |= k; result = INTERSECT; }

       } return result;
}
```

2.6 Octant test

In this optimization method *Möller et al.* used the symmetry of the VF. If the radius of the sphere bounding the AABB is smaller than the smallest distance of the VF plane from the center of the symmetric pyramid then the test with only three planes of the octant, where the AABB center lies, is needed. The situation is in *Figure 7*.

Möller et al. do not give more detailed description of the implementation so we could not implement the octant test to be as good as the authors present. The problem is that the octant that the AABB center belongs to could be determined only by three dot products. This means permanent loss of nine multiplications before the test with the first plane. The next problem is the test of the functionality of the octant test. The comparison of two distances are needed that are computed after any change in the geometry of the AABB and the VF. These computations are called heavily in dynamic scenes so after the activating of this test the VFC is slowed down. Because of this we do not find this test useful and we will not introduce its relatively complicated implementation.
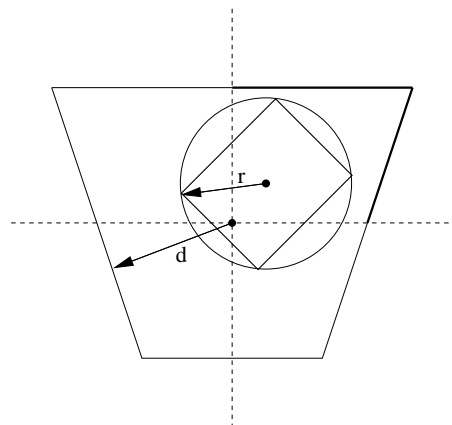

Figure 7: Octant test.

2.7 Translation and rotation coherency

This optimization significantly affects the degree of freedom of the camera and can be used only in the case where none of the AABBs did not move or rotate and when the VF movement is controlled by the user using only simple translations and rotations. It cannot be applied on general walk-through dynamic scenes where the translation and rotation of the camera is is fluently changed. *Villi Miettinen* [6] verified that *TR-coherency* achieves not so good results as *Assarson* and *Möller* presented. We have not implemented this method but the description is presented here. See *Figure 8*:
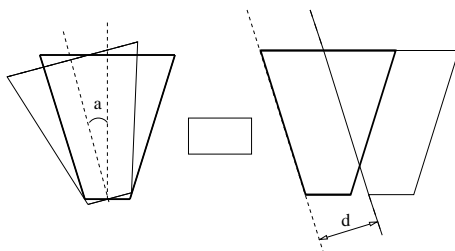

Figure 8: Examples of *TR-coherency*.

- *rotation coherency*: If in the last frame the bounding volume is outside the left plane and the whole rotation of the camera was only to the right, we can report that in the current frame this object is also outside the VF. The rotation need to be less than $180° - \alpha$ where α is the angle between the left and right plane of the VF.
- *translation coherency*: Assume that VF only translated after the last frame and the distances of the VF and the bounding volumes changed by a little Δd. We compute the projection of this increment to the directions of the normal vectors of all VF planes. Before the test for a collision of the given bounding volume with the VF plane we compare the distance to the given plane from the last frame with the current increment. If the increment is greater than this distance the collision detection with the given plane has to be processed.

2.8 Analogy of VFC with the collision detection

The collision test with the VF and the AABB can by easily transformed to the test of two AABBs. In practice, only the plane masking and the plane coherency can help. Speed-up is based only on eliminating several comparisons. The collision test of two AABBs can be done in the six comparisons so a big speed-up could not be expected. Much better optimization could be expected in the test for collision of the two OBBs where the general collision detection is very complex.

3. Our implementation

For verifying the efficiency of the optimization we developed an application that can load hierarchical scenes with a camera and animation, process objects and camera motion, correctly traverse a scene hierarchy, constructs bounding volumes and visualizes the results of tests from the viewpoint including real time measuring.

As an input the internal format of the *3D Studio 4.0* was chosen. It has all necessary properties mainly for scene motion. The application supports animation based on the interpolation of the quaternions using *Kochanek-Bartels* piece-wise continuous spline functions. The hierarchy of the AABBs is automatically actualized. The AABB hierarchy is generated from the current OBB leafs by a transformation.
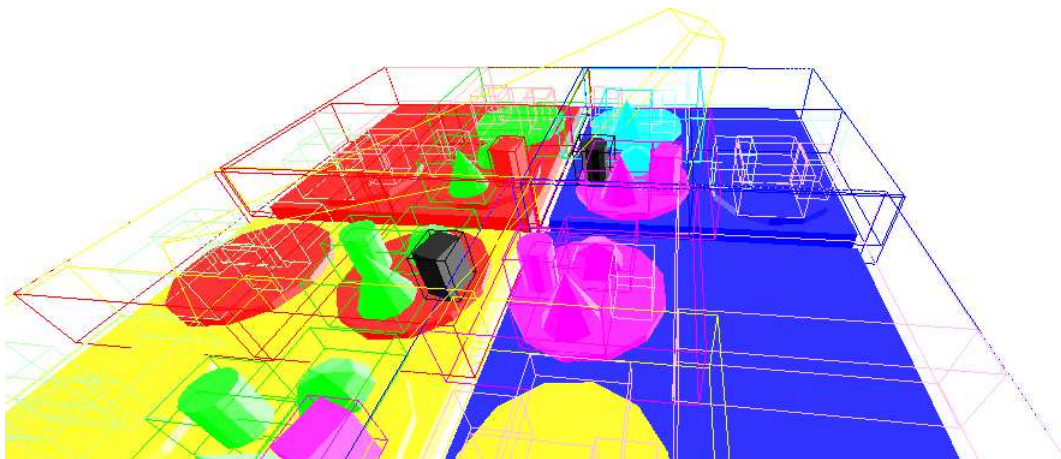

Figure 9: Example output from our application.

The user can watch the scene from the point above the scene or directly by the view of the tested camera. All eight degrees of freedom and the geometry can be controlled by a mouse or by hot keys. The current state of the VFC algorithm can be seen in the output window (see *Figure 9*). Each of the six camera planes has its own color that is used for coloring the objects that collide with this plane. Objects inside the VF are of white color and objects outside are not displayed at all. The current used level of the hierarchy can be seen on the displayed AABBs. The algorithm can be switched to the collision detection mode where the VFC test is applied to the bounding box chosen by a user.
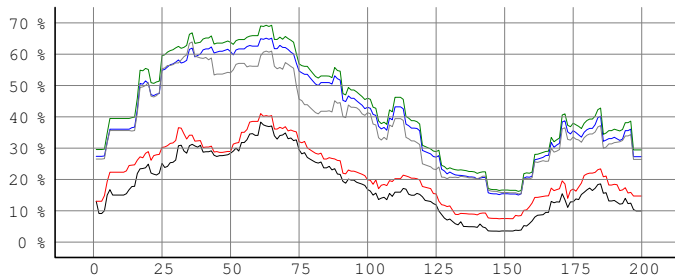
The OpenGL application was compiled using *GCC 3.0* under *Linux* and *Windows* (*MinGW 1.1*). For measurement reasons more functions with different optimization are run simultaneously and the time is measured for each of them. The obtained results is then sent using *TCP/IP* to the independent application (it can be on another computer) that takes care about their processing and displaying.

4. Measurement and results

The efficiency of the optimization was verified on two tested scenes. Both are fully motion, contain simple geometric solids (sphere, cylinder, box and pyramid) in the hierarchy. The first scene (`vfc.3ds`) is smaller in the number of triangles and the camera flies over the entire scene. The second scene (`big.3ds`) is more complex. The camera flies over the entire scene and in one case even outside it.

The measurement was processed in two modes. The first mode (see *Graph 1* and *Graph 3*) represents the influence of a motion of the camera and the objects movement on the VFC efficiency. In the second mode (see *Graph 2* and *Graph 4*) the animation of the objects is disabled in the whole scene. All measurements were performed in the 200-frames animation where in each of the frame different optimization of the VFC algorithm were applied. The measured time is shown relative to the time of the basic VFC algorithm without any hierarchy. The results are in the graphs where is shown time dependency and in the tables where there are the average values for the entire measurement.

4.1 Results from the `vfc.3ds` scene

basic VFC algorithm	43.37%
n,p-vertex test	40.73%
+octant test	38.04%
+plane coherency	22.11%
+plane masking	18.12%

Graph 1: `vfc.3ds` - full objects motion.

basic VFC algorithm	39.35%
n,p-vertex test	37.04%
+octant test	34.47%
+plane coherency	18.10%
+plane masking	14.59%
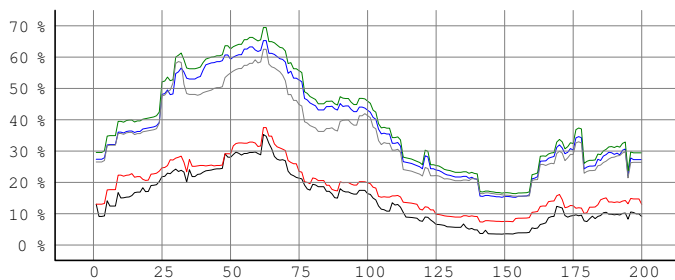
Graph 2: `vfc.3ds` - without animation.

4.2 Results from the `big.3ds` scene

basic VFC algorithm	50.72%
n,p-vertex test	47.61%
+octant test	44.24%
+plane coherency	31.76%
+plane masking	25.41%
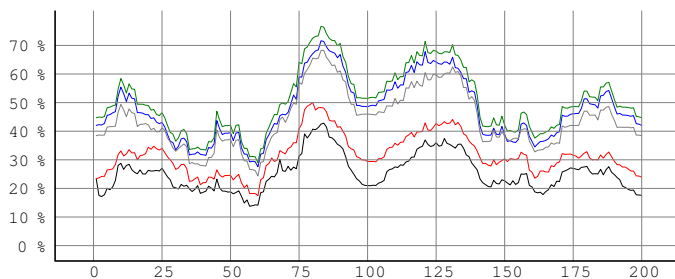
Graph 3: `big.3ds` - full objects motion.

basic VFC algorithm	46.39%
n,p-vertex test	43.61%
+octant test	40.73%
+plane coherency	28.07%
+plane masking	22.39%
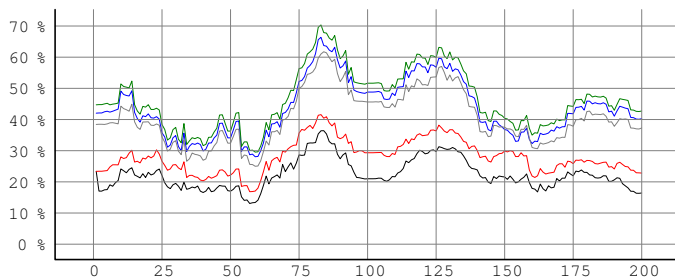
Graph 4: `big.3ds` - without animation.

5. Conclusion

The results show that the best acceleration was reached using the plane coherency of the VF as was theoretically predicted. The presented reasons caused that the results of *Assarson* and *Möller* were not reproduced. The results show how important is the scene hierarchy. The graphs of the speed-up with relation to time proves inefficiency of our implementation of the octant test. On average we provide 2–3 times faster solution compared to the basic algorithm. In the case of static scenes the results of optimization are better then in the case of dynamic scenes as expected. We have verified even the possibility of using of the shown optimization for the collision detection. The side effect of our work is visualization of the VFC algorithm that can be used for the teaching purposes.

6. References

[1] Ulf Assarson and Tomas Möller. Optimized View Frustum Culling Algorithms for Bounding Boxes. In *Journal of Graphics Tools*, 5(1), pages 9–22, 2000.

[2] James H. Clark. Hierarchical Geometric Models for Visible Surface Algorithms. In *Communications of the ACM* 19(10), pages 547–554, 1976.

[3] Mel Slater and Yiorgos Chrysanthou. View Volume Culling Using a Probabilistic Caching Scheme. In *Proceedings of the ACM Symposium on Virtual Reality Software and Technology*, pages 71–78, 1997.

[4] Jiří Bittner and Vlastimil Havran, Exploiting Temporal and Spatial Coherence in Hierarchical Visibility Algorithms. In *Proceedings of Spring Conference on Computer Graphics*, Budmerice, SK, 2001.

[5] Ulf Assarson and Tomas Möller. Optimized View Frustum Culling Algorithms (technical report 99-3). Chalmers University of Technology, Sweden 1999.

[6] Villi Miettinen. Improved frustum-object cull. In *Sourceforge mailing list*, gdAlgorithms-list, 2000.

[7] J.T. Klosowski, M. Held, J.S.B. Mitchell, H. Sowizral and K. Zikan. Efficient Collision Detection Using Bounding Volume Hierarchies of k-DOP. In *IEEE Transactions on Visualization and Computer Graphics*, 4(1), pages 21–36, 1998.